

Raman scattering study of two-dimensional magnetic van der Waals compound VI_3

Yi-Meng Wang(王艺朦), Shang-Jie Tian(田尚杰), Cheng-He Li(李承贺), Feng Jin(金峰), Jian-Ting Ji(籍建葶), He-Chang Lei(雷和畅), Qing-Ming Zhang(张清明)

Citation: Chin. Phys. B . 2020, 29(5): 056301 . **doi:** 10.1088/1674-1056/ab8215
Journal homepage: http://cpb.iphy.ac.cn; http://iopscience.iop.org/cpb

What follows is a list of articles you may be interested in

Raman scattering study of magnetic layered MPS_3 crystals (*M*=Mn, Fe, Ni)

Yi-Meng Wang(王艺朦), Jian-Feng Zhang(张建丰), Cheng-He Li(李承贺), Xiao-Li Ma(马肖莉), Jian-Ting Ji(籍建葶), Feng Jin(金峰), He-Chang Lei(雷和畅), Kai Liu(刘凯), Wei-Lu Zhang(张玮璐), Qing-Ming Zhang(张清明)

Chin. Phys. B . 2019, 28(5): 056301 . **doi:** 10.1088/1674-1056/28/5/056301

Magnetism and piezoelectricity of hexagonal boron nitride with triangular vacancy

Lu-Si Zhao(赵路丝), Chun-Ping Chen(陈春平), Lin-Lin Liu(刘林林), Hong-Xia Yu(于洪侠), Yi Chen(陈怡), Xiao-Chun Wang(王晓春)

Chin. Phys. B . 2018, 27(1): 016301 . **doi:** 10.1088/1674-1056/27/1/016301

Raman phonons in multiferroic $FeVO_4$ crystals

Zhang An-Min, Liu Kai, Ji Jian-Ting, He Chang-Zhen, Tian Yong, Jin Feng, Zhang Qing-Ming

Chin. Phys. B . 2015, 24(12): 126301 . **doi:** 10.1088/1674-1056/24/12/126301

Effect of Gd doping on the magnetism and work function of $Fe_{1-x}Gd_x$/Fe (001)

Tang Ke-Qin, Zhong Ke-Hua, Cheng Yan-Ming, Huang Zhi-Gao

Chin. Phys. B . 2014, 23(5): 056301 . **doi:** 10.1088/1674-1056/23/5/056301

Effect of 6H-SiC (1120) substrate on epitaxial graphene revealed by Raman scattering

Lin Jing-Jing, Guo Li-Wei, Jia Yu-Ping, Chen Lian-Lian, Lu Wei, Huang Jiao, Chen Xiao-Long

Chin. Phys. B . 2013, 22(1): 016301 . **doi:** 10.1088/1674-1056/22/1/016301

Raman scattering study of two-dimensional magnetic van der Waals compound VI_3*

Yi-Meng Wang(王艺朦)[1], Shang-Jie Tian(田尚杰)[1], Cheng-He Li(李承贺)[1], Feng Jin(金峰)[2], Jian-Ting Ji(籍建葶)[2], He-Chang Lei(雷和畅)[1], and Qing-Ming Zhang(张清明)[2,3,†]

[1] *Department of Physics and Beijing Key Laboratory of Opto-electronic Functional Materials & Micro-nano Devices, Renmin University of China, Beijing* 100872, *China*

[2] *Beijing National Laboratory for Condensed Matter Physics, Institute of Physics, Chinese Academy of Sciences, Beijing* 100190, *China*

[3] *School of Physical Science and Technology, Lanzhou University, Lanzhou* 730000, *China*

(Received 8 February 2020; revised manuscript received 9 March 2020; accepted manuscript online 23 March 2020)

The layered magnetic van der Waals materials have generated tremendous interest due to their potential applications and importance in fundamental research. Previous x-ray diffraction (XRD) studies on the magnetic van der Waals compound VI_3, revealed a structural transition above the magnetic transition but output controversial analysis on symmetry. In this paper we carried out polarized Raman scattering measurements on VI_3 from 10 K to 300 K, with focus on the two A_g phonon modes at ~ 71.1 cm^{-1} and 128.4 cm^{-1}. Our careful symmetry analysis based on the angle-dependent spectra demonstrates that the crystal symmetry can be well described by C_{2h} rather than D_{3d} both above and below structural phase transition. We further performed temperature-dependent Raman experiments to study the magnetism in VI_3. Fano asymmetry and anomalous linewidth drop of two A_g phonon modes at low temperatures, point to a significant spin–phonon coupling. This is also supported by the softening of 71.1-cm^{-1} mode above the magnetic transition. The study provides the fundamental information on lattice dynamics and clarifies the symmetry in VI_3. And spin–phonon coupling existing in a wide temperature range revealed here may be meaningful in applications.

Keywords: Raman scattering, two-dimensional magnetic van der Waals materials, lattice dynamics, magnetism

PACS: 63.20.–e, 63.22.–m, 75.75.–c, 78.30.–j **DOI:** 10.1088/1674-1056/ab8215

1. Introduction

Two-dimensional (2D) magnetism is always a very broad and fundamentally interesting topic in condensed matter physics. One of the current research hotspots is to search for single-layer magnetic materials exfoliated from a bulk that possesses a robust magnetic order.[1–5] Recent studies focus on a number of potentially 2D van der Waals (vdW) magnetic materials, including binary transition metal halides MX_y (M = metal cation; X = halogen anion),[6,7] chromium based CrOCl,[8–12] and transition-metal (TM) phosphorous trichalcogenides MPX_3 (M denotes TM atoms; X = S or Se).[3,13–17] Both VI_3 and CrI_3 belong to the MX_3 trihalide family.[18–23] CrI_3 has been extensively studied[1,2,24–26] in the last few years and more and more attention is paying to VI_3 now. Generally V compounds have more complicated physical properties compared to Cr compounds. Recently single crystals of VI_3 have been grown and some basic physical properties were measured.[27–32] However, spectroscopic studies are still highly required.

VI_3 has the layered BiI_3-type structure with VI_6 octahedra sharing edges in each layer to form a honeycomb lattice and exhibits a structural phase transition at $T_s \sim 79$ K.[27] VI_3 is a typical semiconductor and has a long-range ferromagnetic (FM) ordering at $T_c \sim 50$ K.[27] Previous studies on the crystal structure gave controversial results and no consensus has been reached yet. XRD refinements suggested two distinct high-temperature phases $P31c$[29] and $C2/m$[27] respectively, while $R\bar{3}$[27] and $C2/c$[29] space groups were proposed as the corresponding low-temperature phases below the structural transition. Clearly one can clarify the symmetry by distinguishing the point group. That is exactly one of the outstanding advantages Raman scattering possesses. This motivates us to perform polarized Raman scattering measurements to determine the point symmetry across the structural transition. The rich magnetism reported in VI_3 also allows us to look into the spin-related excitations/interactions by performing temperature-dependent Raman scattering experiments.

In this paper, we have performed polarized and temperature-dependent Raman scattering measurements on VI_3. The angle-dependent Raman spectra indicate that the point group C_{2h} remains unchanged from ~ 10 K to 300 K, ruling out D_{3d} symmetry. The temperature-dependent Raman spectra of the two A_g phonon modes at 71.1 cm^{-1} and 128.4 cm^{-1} catch the signature of the structural phase tran-

*Project supported by the Science Fund from the Ministry of Science and Technology of China (Grant Nos. 2017YFA0302904 and 2016YFA0300504), the National Natural Science Foundation of China (Grant Nos. 11774419, U1932215, 11774423, and 11822412), the Fundamental Research Funds for the Central Universities, China, and the Research Funds of Renmin University of China (RUC) (Grant Nos. 15XNLQ07, 18XNLG14, and 19XNLG17).

†Corresponding author. E-mail: qmzhang@ruc.edu.cn

© 2020 Chinese Physical Society and IOP Publishing Ltd

sition. The sharp tendency of the linewidth and Fano asymmetry for both modes suggest a clear spin–phonon coupling. The abnormal behavior of 71.1-cm^{-1} mode in frequency also confirms the spin–phonon coupling.

2. Experimental methods

VI_3 single crystals used in this study were grown using the chemical vapor transport method (CVT). The details of crystal growth can be found elsewhere.[27] We obtained the glossy crystals with flat surface and then quickly transferred the sample into a UHV cryostat with a vacuum of better than 10^{-8} mbar (1 bar = 10^5 Pa). The polarized and angular Raman spectra and temperature-dependent Raman spectra were collected using a HR800 spectrometer (Jobin Yvon) equipped with a liquid-nitrogen-cooled charge-coupled device (CCD) and volume Bragg gratings, and micro-Raman backscattering configuration was adopted. A 633-nm laser was used with a spot size of ~ 5 μm focused on sample surface. The scattered signal was collected through a 50× long focus-length objective, and dispersed with a 600-grooves/mm grating. The laser power was maintained at approximately ~ 1.4 mW to avoid overheating the sample during measurements. The angle dependence of mode intensities was measured by rotating light polarizations with careful adjustment of the angle matching. We define X and Y axes in the crystallographic ab plane. X is perpendicular to the b axis and Y is along the b axis. Z is perpendicular to X and Y. The incident light direction was perpendicular to the (001) plane.

3. Results and discussions

Previous x-ray diffraction studies proposed two distinct high-temperature structural phases $C2/m$[27] and $P31c$,[29] which change to low-temperature phases $R\bar{3}$[27] and $C2/c$[29] after the structural transition, respectively. $P31c$ belongs to D_{3d} point group while $C2/m$ and $C2/c$ share C_{2h} point group symmetry. The symmetry issue can be solved by determining the point group symmetry. That is exactly what Raman scattering can do.

For C_{2h} point group, there are $8A_g + 7B_g$ Raman active modes at the Γ point. The corresponding Raman tensors are

$$A_g = \begin{pmatrix} b & 0 & d \\ 0 & c & 0 \\ d & 0 & a \end{pmatrix}, \quad B_g = \begin{pmatrix} 0 & f & 0 \\ f & 0 & e \\ 0 & e & 0 \end{pmatrix}.$$

This gives rise to the different angular dependences of the phonon intensity $I(\theta)$ for the A_g and B_g modes when the incident/scattered light polarizations (e_i/e_s) is rotated in the ab plane,

$$\begin{aligned} e_i \parallel e_s: \quad & A_g: I(\theta) = \left[b\sin^2\theta + c\cos^2\theta\right]^2, \\ & B_g: I(\theta) = \left[e\sin(2\theta)\right]^2, \end{aligned} \tag{1}$$

$$\begin{aligned} e_i \perp e_s: \quad & A_g: I(\theta) = \left[\frac{(b-c)}{2}\sin(2\theta)\right]^2, \\ & B_g: I(\theta) = \left[e\cos(2\theta)\right]^2, \end{aligned} \tag{2}$$

where θ is defined as the angle between e_i and Y axis. From Eqs. (1) and (2), we can see that when $\theta = 0$, A_g mode only appears under parallel polarization and B_g mode only appears under cross polarization. And one can expect that A_g mode will have a four-fold symmetry under cross polarization.

On the other hand, for D_{3d} point group, there are $3A_{1g} + 5E_g$ Raman active modes at the Γ point. The corresponding Raman tensors are

$$A_{1g} = \begin{pmatrix} a & 0 & 0 \\ 0 & a & 0 \\ 0 & 0 & b \end{pmatrix}, \quad E_{g,1} = \begin{pmatrix} c & 0 & 0 \\ 0 & -c & d \\ 0 & d & 0 \end{pmatrix},$$
$$E_{g,2} = \begin{pmatrix} 0 & -c & -d \\ -c & 0 & 0 \\ -d & 0 & 0 \end{pmatrix}.$$

In this case, the intensity of A_{1g} mode remains unchanged with rotation in parallel polarization while it is always zero in cross polarization. The clear contrast of phonon intensity evolution with angle provides a unique opportunity to distinguish the crystal symmetry.

In Fig. 1 we show Raman spectra of VI_3 at 10 K and 300 K. There are two well-defined modes located at 71.1 cm^{-1} and 128.4 cm^{-1} at 300 K. The two modes only appear in parallel polarization and can be assigned to A_g modes according to the symmetry analyses above. The emergence of the 98.0-cm^{-1} phonon mode at 10 K is an indication of thermal broadening reduction at low temperatures, rather than a phase transition. This is confirmed by its continuous evolution in intensity from 10 K to 300 K. The optical modes in CrI_3 have been calculated.[33,34] VI_3 has exactly the same crystal symmetry with CrI_3 and hence the 98-cm^{-1} mode in VI_3 can be safely attributed to the mode ~ 101.9 cm^{-1} in CrI_3 based on the energy and symmetry. The A_g mode in both VI_3 and CrI_3 represents the joint vibrations of magnetic ions and I^- anions.

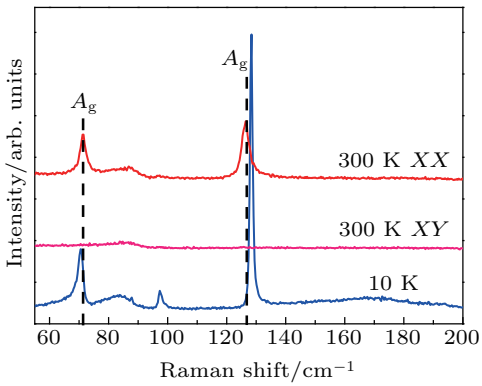


Fig. 1. Polarized Raman spectra in VI_3 at 300 K under $Z(XX)\bar{Z}$ (red line) and $Z(XY)\bar{Z}$ (pink line) scattering geometries. The phonon modes at 71.1 cm^{-1} and 128.4 cm^{-1} are A_g ones. Unpolarized Raman spectrum at 10 K is also shown here.

To look into the crystal symmetry at 10 K and 300 K, we analyze the angular dependence of the intensities of the two A_g modes at 71.1 cm^{-1} and 128.4 cm^{-1}. In Figs. 2(b) and 2(c), we track the angular dependence of their intensities under cross polarizations at 10 K and 300 K. In cross channel at 300 K, the intensities of the two modes are non-zero and the crystal exhibits a four-fold symmetry. This tells us that the crystal symmetry of VI_3 at 300 K is C_{2h} point group if we check it with Eq. (2). Similarly, the two modes are still non-zero and the four-fold symmetry remains at 10 K. The small deviation between the experimental data and the fitting curve results from the vibration of the sample stage at low temperatures and has little effect on symmetry analysis. As the VI_6 octahedra experience an off-center distortion with the low temperature which will decrease the symmetry of crystal, the single crystal still keeps the symmetry of C_{2h} point group at 10 K rather than $R\bar{3}$ with a higher symmetry. The interlayer coupling in VI_3 is much stronger than that in the MPX_3 family. This implies that the bulk VI_3 at room temperature may not be simply described using D_{3d} point group.[35]

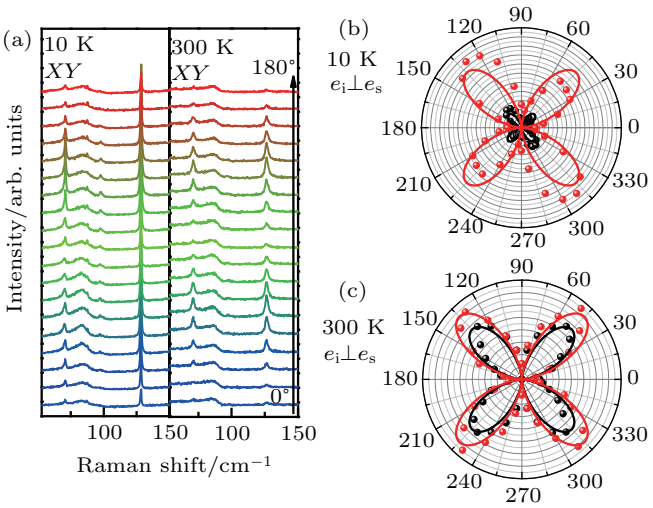


Fig. 2. (a) Raman spectra in cross polarization configuration ($e_i \perp e_s$) collected by rotating light polarizations at 10 K and 300 K. (b) and (c) Intensity plots with respect to the rotation angle for A_g modes in cross channel ($e_i \perp e_s$) at 10 K and 300 K, respectively. The red (black) dots are the experimental data of 128.4 cm^{-1} (71.1 cm^{-1}) modes and the solid curves are fitting curves using the intensity functions (2). The e_i and e_s represent the polarizations of the incident and scattered light, respectively.

We further performed temperature-dependent Raman measurements to study the structural phase transition and magnetic properties in VI_3. In general, for anharmonic phonon modes, the phonon frequencies ω and the linewidths Γ as a function of temperature are given by[36]

$$\omega(T) = \omega_0 - B\left(\frac{2}{e^{\hbar\omega/k_BT} - 1}\right), \quad (3)$$

$$\Gamma(T) = \Gamma_0 - C\left(\frac{2}{e^{\hbar\omega_0/k_BT} - 1}\right), \quad (4)$$

where ω_0 is the bare phonon frequency.

The frequency shift ω and the linewidth Γ of 128.4-cm^{-1} A_g mode as a function of temperature are extracted from Fig. 3(a) and shown in Figs. 3(b) and 3(c), respectively. It can be seen that there is a frequency turn up accompanied by a drop linewidth, near structural phase transition. The anharmonic fitting is applied to the temperature ranges above and below T_s, respectively. Clearly the anomalies are caused by the structural phase transition. Besides the structural transition, it is also reported that VI_3 has an FM phase transition at $\sim$ 50 K.

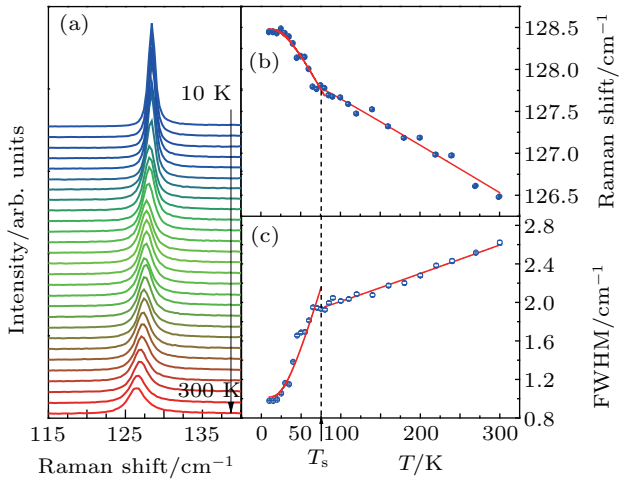


Fig. 3. (a) Temperature dependence of 128.4-cm^{-1} A_g mode. Temperature dependence of frequency shift (b) and linewidth (c) of the A_g mode (left axis). The solid red lines in panel (b) represent the fits with Eq. (3) and the lines in panel (c) represent the fits with Eq. (4).

An interesting observation is that the two A_g modes at $\sim$ 71.1 cm^{-1} and 128.4 cm^{-1}, display a pronounced Fano asymmetry at low temperatures ($T < T_c$) and vanishes for $T > T_c$, as shown in Figs. 3(a) and 4(a). As a semiconductor with a bandgap of $\sim$ 0.9 eV,[27] the electron–phonon coupling effect is expected to be small. The Fano asymmetry may stem from the spin–phonon coupling.

Figures 4(b) and 4(c) show the frequency shift ω and the linewidth Γ of 71.1 cm^{-1} as a function of temperature. There is also a turn point for the mode. The frequencies and linewiths have a small anomaly near $T_s \sim 79$ K, which is considered to be a signature of structural phase transition. The rapid narrowing in phonon linewidth becomes below $T_c \sim 50$ K, indicates that spin–phonon coupling exist in VI_3. In addition, 71.1-cm^{-1} mode exhibits an unusual softening above the magnetic transition and goes back to the normal anharmonic behavior below the magnetic transition. This implies that 71.1-cm^{-1} mode has a stronger spin-coupling than 128.4-cm^{-1} phonon. The frequency of A_g phonon at 71.1 cm^{-1} is lower, which is dominated by the vibration of magnetic ions V^{3+}. It may explain why the phonon softening caused by the spin–phonon coupling in 71.1-cm^{-1} phonon is more significant than that in 128.4-cm^{-1} phonon. The spin–phonon coupling existing

in such a large temperature range in VI_3 will be essential for wide applications.

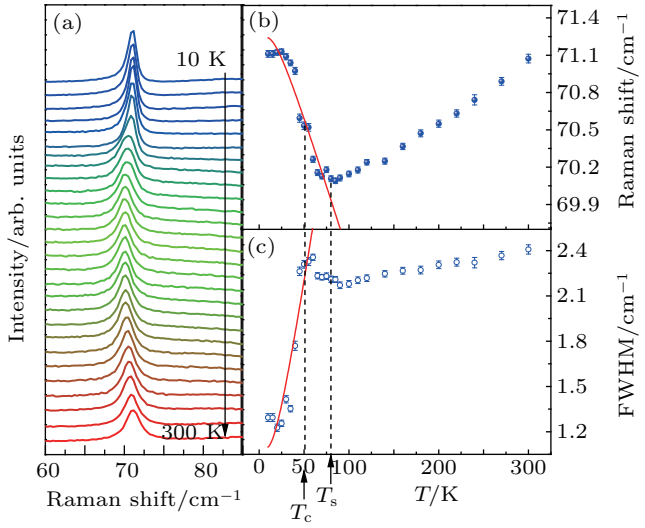


Fig. 4. (a) Temperature dependence of Raman spectra of 71.1-cm^{-1} A_g mode. Temperature dependence of frequency shift (b) and linewidth (c) (left axis). The solid red lines in panels (b) and (c) represent the fits with Eq. (3) and Eq. (4).

4. Conclusion

In summary, we have carried out angle- and temperature-dependent Raman scattering measurements on VI_3 single crystals. The polarized Raman spectra indicate that the crystal symmetry at 10 K and 300 K can be described by C_{2h} rather than D_{3d} point group. The signatures of the structural phase transition are observed in the temperature-dependent Raman spectra. And interestingly, the clear asymmetry of the two A_g modes and the softening of the 71.1-cm^{-1} mode evidence a significant spin–phonon coupling in the system. These observations clarify the symmetry issue on the structural transition and reveal the spin–phonon coupling which may be of interest for potential applications.

References

[1] Huang B, Clark G, Moratalla E N, Klein D R, Cheng R, Seyler K L, Zhong D, Schmidgall E, McGuire M A, Cobden D H, Yao W, Xiao D, Herrero P J and Xu X D 2017 *Nature* **546** 270

[2] Jin W C, Kim H H, Ye Z P, Li S W, Rezaie P, Diaz F, Siddiq S, Wauer E, Yang B, Li C H, Tian S J, Sun K, Lei H C, Tsen A W, Zhao L Y and He R 2018 *Nat. Comm.* **9** 5122

[3] Kuo C T, Neumann M, Balamurugan K, Park H J, Kang S, Shiu H W, Kang J H, Hong B H, Han M, Hoh T W and Park J G 2016 *Sci. Rep.* **6** 20904

[4] Kim K, Lim S Y, Lee J U, Lee S, Kim T Y, Park K, Jeon G S, Park C H, Park J G and Cheong H 2019 *Nat. Comm.* **10** 345

[5] Ozcan M, Ozen S, Yagmurcukardes M and Sahin H 2020 *J. Magn. Magn. Mater.* **493** 165668

[6] McGuire M A 2017 *Crystals* **7** 121

[7] Iyikanat F, Yagmurcukardes M, Senger R T and Sahin H 2018 *J. Mater. Chem. C* **6** 2019

[8] Wang M X, Zhang J, Wang Z P, Wang C, van Smaalen S, Xiao H, Chen X, Du C L, Xu X G and Tao X T 2019 *Adv. Opt. Mater.* **8** 901446

[9] Angelkort J, Wölfel A, Schönleber A, Smaalen S V and Kremer K R 2009 *Phys. Rev. B* **80** 144416

[10] Bykov M, Bykova E, Dubrovinsky L, Hanfland M, Liermann H P and Smaalen S V 2015 *Sci. Rep.* **5** 9647

[11] Miao N H, Xu B, Zhu L G, Zhou J and Sun Z M 2018 *J. Am. Chem. Soc.* **140** 2417

[12] Zhang T L, Wang Y M, Li H X, Zhong F, Shi J, Wu M H, Sun Z Y, Shen W F, Wei B, Hu W D, Liu X F, Huang L, Hu C G, Wang Z C, Jiang C B, Yang S X, Zhang Q M and Qu Z 2019 *ACS Nano* **13** 11353

[13] Lee J, Lee S, Ryoo J H, Kang S, Kim T Y, Kim P, Park C, Park J and Cheong H 2016 *Nano Lett.* **16** 7433

[14] Murayama C, Okabe M, Urushihara D, Asaka T, Fukuda K, Isobe M, Yamamoto K and Matsushita Y 2016 *J. Appl. Phys.* **120** 142114

[15] Wang X Z, Du K Z, Liu Y Y F, Hu P, Zhang J, Zhang Q, Owen M H S, Lu X, Gan C K, Sengupta P, Kloc C and Xiong Q H 2016 *2D Mater.* **3** 031009

[16] Li X, Cao T, Niu Q, Shi J and Feng J 2013 *Proc. Natl. Acad. Sci. USA* **110** 3738

[17] Frindt R F, Yang D and Westreich P 2005 *J. Mater. Res.* **20** 1107

[18] Juza D, Giegling D and Schäfer H 1969 *Z. Anorg. Allg. Chem.* **366** 121

[19] Dillon J and Olson C 1965 *J. Appl. Phys.* **36** 1259

[20] Wilson J, Maule C, Strange P and Tothill J 1987 *J. Phys. C* **20** 4159

[21] Starr C, Bitter F and Kaufmann A R 1940 *Phys. Rev.* **58** 977

[22] Zhou Y G, Lu H F, Zu X T and Gao F 2016 *Sci. Rep.* **6** 19407

[23] He J, Ma S, Lyu P and Nachtigall P 2016 *J. Mater. Chem. C* **4** 2518

[24] Wang H, Fan F, Zhu S and Wu H 2016 *Europhys. Lett.* **114** 47001

[25] Lado J L and Fernández R J 2017 *2D Mater.* **4** 035002

[26] Zhong D, Seyler K L, Xia Y, Lin P, Cheng R, Sivadas N, Huang B, Schmidgall E, Taniguchi T, Watanabe K, McGuire M A, Wang Y, Xiao D, Fu C K M and Xu X D 2017 *Sci. Adv.* **3** e1603113

[27] Tian S, Zhang J F, Li C, Ying T, Li S, Zhan X, Liu K and Lei H 2019 *J. Am. Chem. Soc.* **141** 5326

[28] Kong T, Stolze K, Timmons E I, Tan J, Ni D, Guo S, Yang Z, Prozorov R and Cava R J 2019 *Adv. Mater.* **31** 1808074

[29] Son S, Coak M J, Lee N, Kim J, Kim T Y, Hamidov H, Cho H, Liu C, Jarvis D M, Brown P A C, Kim J H, Park C, Khomskii D I, Saxena S S and Park J 2019 *Phys. Rev. B* **99** 041402

[30] Liu Y, Abeykoon M and Petrovic C 2020 *Phys. Rev. Res.* **2** 013013

[31] An M, Zhang Y, Chen J, Zhang H M, Guo Y and Dong S 2019 *J. Phys. Chem. C* **123** 30545

[32] Askurt M, Eren I, Yagmurcukardes M and Sahin H 2020 *Appl. Surf. Sci.* **508** 144937

[33] Larson D T and Kaxiras E 2018 *Phys. Rev. B* **98** 085406

[34] Djurdjić-Mijin S, Šolajić A, Pešić J, Šćepanović M, Liu Y, Baum A, Petrovic C, Lazarević N and Popović Z V 2018 *Phys. Rev. B* **98** 104307

[35] Wang Y M, Zhang J F, Li C C, Ma X L, Ji J T, Jin F, Lei H C, Liu K, Zhang W L and Zhang Q M 2019 *Chin. Phy. B* **28** 056301

[36] Djokić D M, Popović Z V and Vukajlović F R 2008 *Phys. Rev. B* **77** 014305